Environmental Science and Ecotechnology 16 (2023) 100276

Contents lists available at ScienceDirect

Environmental Science and Ecotechnology

journal homepage: www.journals.elsevier.com/environmental-science-and-ecotechnology/

Influence of carbon-based cathodes on biofilm composition and electrochemical performance in soil microbial fuel cells

Arpita Nandy [a], Daniel Farkas [b], Belén Pepió-Tárrega [c], Sandra Martinez-Crespiera [c], Eduard Borràs [c], Claudio Avignone-Rossa [b], Mirella Di Lorenzo [a, *]

[a] Department of Chemical Engineering and Centre for Biosensors, Bioelectronics & Biodevices (C3Bio), University of Bath, Claverton Down, BA2 7AY, UK
[b] Department of Microbial Sciences, University of Surrey, Guildford, GU2 7XH, UK
[c] LEITAT Technological Center, C/ de la Innovació, 2, 08225, Terrassa, Barcelona, Spain

ARTICLE INFO

Article history:
Received 21 October 2022
Received in revised form
30 March 2023
Accepted 3 April 2023

Keywords:
Soil microbial fuel cells
ORR catalyst
Carbon nanofibre
Microbial profiling

ABSTRACT

Increasing energy demands and environmental pollution concerns press for sustainable and environmentally friendly technologies. Soil microbial fuel cell (SMFC) technology has great potential for carbon-neutral bioenergy generation and self-powered electrochemical bioremediation. In this study, an in-depth assessment on the effect of several carbon-based cathode materials on the electrochemical performance of SMFCs is provided for the first time. An innovative carbon nanofibers electrode doped with Fe (CNFFe) is used as cathode material in membrane-less SMFCs, and the performance of the resulting device is compared with SMFCs implementing either Pt-doped carbon cloth (PtC), carbon cloth, or graphite felt (GF) as the cathode. Electrochemical analyses are integrated with microbial analyses to assess the impact on both electrogenesis and microbial composition of the anodic and cathodic biofilm. The results show that CNFFe and PtC generate very stable performances, with a peak power density (with respect to the cathode geometric area) of 25.5 and 30.4 mW m^{-2}, respectively. The best electrochemical performance was obtained with GF, with a peak power density of 87.3 mW m^{-2}. Taxonomic profiling of the microbial communities revealed differences between anodic and cathodic communities. The anodes were predominantly enriched with *Geobacter* and *Pseudomonas* species, while cathodic communities were dominated by hydrogen-producing and hydrogenotrophic bacteria, indicating H_2 cycling as a possible electron transfer mechanism. The presence of nitrate-reducing bacteria, combined with the results of cyclic voltammograms, suggests microbial nitrate reduction occurred on GF cathodes. The results of this study can contribute to the development of effective SMFC design strategies for field implementation.

1. Introduction

Renewable energy is the only answer to balance increasing global energy demands with the net-zero emissions target by 2050. It is unlikely that one single approach could solve such a great challenge and help minimise our dependence on fossil fuels. Therefore, the most promising strategy is to explore the synergistic contribution of several green energy systems.

Amongst the different options, microbial electrochemical technologies hold great potential, given their cost-effectiveness and unique ability to degrade organic matter in biological waste with the concomitant production of electrical energy. In this context, soil microbial fuel cell (SMFC) is a particularly attractive carbon-neutral and affordable technology, able to exploit the use of the endogenous microorganisms present in the soil to convert the organic matter in the soil into useful electricity [1]. The estimated number of bacterial species per gram of soil varies between 2000 and 8.3 million [2,3], and the abundance of organic matter, despite the variation between different soil types, is approximately 100 mg g^{-1} [4,5]. These features make the soil a very sustainable source of energy. SMFC technology also offers great opportunities as a self-powered and sustainable *in situ* bioremediation strategy for soils contaminated with metals, hydrocarbons, and pesticides [6].

Contrary to traditional (i.e., liquid-based) microbial fuel cells,

* Corresponding author.
E-mail address: m.di.lorenzo@bath.ac.uk (M. Di Lorenzo).

https://doi.org/10.1016/j.ese.2023.100276

SMFC technology is still in its infancy, with studies mainly focused on assessing its potential for soil bioremediation [7,8]. Nonetheless, SMFCs are characterised by simple, low-cost, and low-maintenance designs, which facilitate translating the technology from the lab to the field [9]. In microbial fuel cells, the electrode material plays an important role in performance. Current generation in such systems is highly dependent on the cathode's reduction kinetics, and in the case of air-cathode designs, the oxygen reduction reaction (ORR) is one of the major limiting factors in electricity generation due to its high activation energy [10,11]. This high energy is traditionally overcome by using platinum as a catalyst, which is expensive and suffers from biofouling effects [12,13]. Many high-performing transition metal-based catalysts (Fe, Co, Ni, etc.) have been developed to provide a low-cost, durable alternative [14–17]. Composite electrode materials, consisting of transition metals supported by a carbon matrix and conductive polymers, have also been proposed [11,17]. To develop cathode materials with high catalytic activity, activated carbon has been functionalised with a metal–organic framework (MOF) [18], while the performance of air cathodes in microbial fuel cells has been enhanced by functionalising activated carbon with reduced graphene oxide [19]. Nanostructure-based carbon materials, such as carbon nanotubes, nanofibers, and graphene, are gaining increasing interest due to their large surface area and functionality [20–22] and, therefore, approaches like doping metal particles on carbon nanostructure are very attractive [23,24]. Carbon nanofibers (CNFs) have been explored for the functionalization of electrodes in microbial fuel cells since they provide very high electrical conductivity, high chemical stability, high porosity, and high specific surface area [23–28]. Electrospinning of CNFs has proven to be more effective in terms of catalytic activity than physical or chemical modification due to the larger surface area achieved [29,30]. Nonetheless, so far, CNFs have been only tested for liquid-fed microbial fuel cells, and, despite their great potential, only very few studies have exploited their benefits [31–35]. Doping CNFs with Ni nanoparticles can lead to high electrical conductivity due to spontaneous nitrogen defects upon treatment at 900 °C; high power density was achieved using these electrodes as the cathode in liquid microbial fuel cells [28]. Table S1 provides an overview of the cathode material used for SMFCs. Typically, in SMFCs, unmodified carbon-based materials, such as carbon felt, carbon cloth, and granular activated carbon, are used as a cathode [36–40]. Nonetheless, carbon-based and stainless steel-based electrodes functionalised with Pt (0.1–0.2 mg cm^{-2}) [41,42] or alternative catalysts, such as Ni, in combination with platinum, have also been reported [43–45]. The power densities obtained with different configurations of SMFCs, such as single chamber [36,44,45], column type [41], tubular [46], or U type [42], are within the range of 0.85–77.5 mW m^{-2} [36,39,40,42], except for few cases where a polymer electrolyte membrane was used in dual chamber microbial fuel cell, in which a value as high as 7.5 mW cm^{-2} was obtained [38]. It is expected that the SMFC performance improves with the use of an ORR catalyst at the cathode, however, the power output generated by SMFCs with a Pt-coated cathode (0.1–0.2 mg cm^{-2}), was reported to be within the range of 8.8–39 mW m^{-2} [41,43,46], while composite electrodes, fabricated by modifying a stainless-steel matrix with conductive carbon black, can lead to power densites over 250 mW m^{-2} with no need for an expensive catalyst [44,45]. Although a proper comparison among the different systems is difficult given the great difference in the design parameters used for each study, it is clear that there is great scope to develop robust and efficient cathodes to improve the performance of SMFCs. In this study, we investigate and compare for the first time the performance of four different cathodes in membrane-free air-cathode SMFCs: carbon cloth (SMFC-CC), Pt-doped carbon cloth (SMFC-PtC), graphite felt (SMFC-GF), and Fe-doped CNFs (SMFC-CNFFe). Electrochemical tests over prolonged operating times are complemented by microbial taxonomic analyses to elucidate the influence that the electrode material has on the cathodic and anodic biofilm formation and, consequently, on the overall electrochemical performance, thus guiding the development of highly performing SMFC designs.

2. Materials and methods

2.1. Materials

The chemicals used in this experiment were purchased from Alfa Aesar/Thermo Fischer Scientific (Lancashire, UK) and Sigma-Aldrich (Merck Life Science UK Limited, Gillingham, UK). Graphite felt was purchased from Online Furnace Services Ltd (Scotland, UK), and carbon cloth doped with Pt and plain carbon cloth were purchased from the Fuel Cell Store (Texas, USA). The soil was collected around the campus area of the University of Bath from a maximum depth of 30 cm below the surface. The soil was cleaned of visible stones, gravel, roots, and leaves before use. The physicochemical properties of the soil were assessed by an external company (Eurofins Chemtest Ltd, New Market, United Kingdom) and resulted as follows: 39% moisture content, 14% total organic carbon, pH 7.2, and electrical conductivity 1090 μS cm^{-1}.

2.2. Preparation of the CNF–Fe cathode

The CNF–Fe cathode fabrication was performed as reported in previous work [23,24]. First, a precursor solution for electrospinning was prepared, which consisted of a polyacrylonitrile (PAN) and polyvinyl pyrrolidone (PVP) solution (9:3 wt ratio, w/w) in 12% w/w N,N-dimethylformamide, DMF, containing 3 mmol of iron acetate $Fe(CH_3COO_2)$. The solution was then electrospun (NF-103, MECC) with a multi-spinneret with three syringes under the following conditions: flow: 2–3 mL h^{-1}; distance: 15 cm; applied potential: 29.9 kV; rotating collector speed: 300 rpm. Finally, a thermal treatment (Carbolite furnace) was applied with an initial heating gradient of 1 °C min^{-1} up to 280 °C (4 h) under air, followed by a second heating gradient of 5 °C min^{-1} up to 1000 °C (1 h) under Ar.

A detailed physicochemical characterization of the CNF–Fe cathode is reported in Table S2 in the supporting information. Morphology analysis was evaluated using a ZEISS MERLIN (Germany) high-resolution field emission scanning electron microscope (FESEM) (Fig. S1), using both secondary electrons (SE) and backscattered electrons (BSE) Electron Microscopy Facilities, at the Universitat Autònoma de Barcelona (UAB, Bellaterra, Spain). The diameter of CNFs and FeNPs was analysed by ImageJ software. To determine specific surface area, total pore volume, and mesoporosity, nitrogen adsorption isotherms at 77 K were recorded with aNova 2200e equipment (Quantachrome Instruments, USA) (Fig. S2). A BET surface analyser was used within the relative pressure range of 0.05–0.2 to assess the specific surface area. The electrical conductivity was measured from the sheet resistance of the electrospun film with a homemade device, as shown in Fig. S3.

2.3. SMFC design and operation

The SMFCs tested in this study were constructed in triplicates and fitted in polypropylene boxes (40 × 26 × 15 cm) filled with soil. No external organic carbon was added to the soil. The SMFCs consisted of an anode buried in the soil and a cathode exposed to air at a fixed electrode distance of 4 cm, which was maintained using nylon screws (Bluemay Limited, Wiltshire, UK), as shown in Fig. 1c. The anode (graphite felt, 7 × 7 × 0.4 cm) was pre-treated to

increase the hydrophilicity and roughness of the carbon nanofibers, as previously described [47]. With regards to the cathode, four different materials were tested; the performance of the Fe-doped CNFs cathode was compared with three commercial materials (Fig. 1a): carbon cloth with Pt (Pt loading: 0.2 mg cm^{-2}), plain carbon cloth, and graphite felt. In each case, the cathode ($7 \times 7 \times 0.4$ cm) was encased between two sheets of titanium mesh (gauze woven from wire 40 mesh, 0.127 mm, VWR), as shown in Fig. 1b, and titanium mesh without any electrode was used as control (Fig. S4). Ti mesh was used to improve the physico-chemical and mechanical properties of the system: imparting mechanical stability to the brittle CNFFe electrodes, allowing better current collection, and reducing cathodic polarization resistance [48]. The anode and cathode were connected to an external resistance of 500 Ω, which was chosen according to our previous standardization experiments with SMFCs [9,49], and to a data acquisition system (DAQ6510, Keithley instruments, Tektronix UK Ltd.) with titanium wire (diameter 0.25 mm, VWR) intertwined within the electrodes. The output voltage was monitored over time at 1-min intervals, howwever, for better data visualization and interpretation, the average of one-day measurements was plotted so that graphs refer to data points at the one-day interval. Individual anode and cathode potentials were also measured everyday with respect to the Ag/AgCl reference electrode. The initial output voltage was very low for the SMFCs until about day 40 due to poor contact between soil and cathodes. To overcome this issue, on day 40 of operation, additional soil was added between the anode and cathode. Data are shown from day 40 of operation onwards, which is indicated as day 0 in the graphs.

2.4. Electrochemical measurements and analyses

Once a steady output voltage was generated, polarization tests on the SMFCs were performed by varying the applied external load from 100 KΩ to 10 Ω with a resistor box. In these tests, the SMFCs were first operated in open circuit voltage (OCV) until a stable voltage was generated (approximately after 1 h) and then connected to a resistor box (Cropico RM6 Decade). The current (I) was calculated using Ohm's law $V=IR$, where R is the applied external resistor, and the power (P) was calculated as $P=IV$. The soil was kept moistened with tap water, which was added daily. Cyclic voltammetry (CV) tests, within the range −1 to +1 V at a scan rate of 5 mV s^{-1}, were performed *in situ* by using the cathode as the working electrode, the anode as the counter electrode, and Ag/AgCl as the reference electrode. Electrochemical Impedance Spectroscopy (EIS) was performed in a two-electrode system, with the cathode as the working electrode and the anode as the counter electrode, at the frequency range 1500 kHz–25 mHz and with an amplitude of the applied signal of 10 mV. The resulting data were analysed using EC-lab® software (V10.40, BioLogic, Seyssinet-Pariset, France).

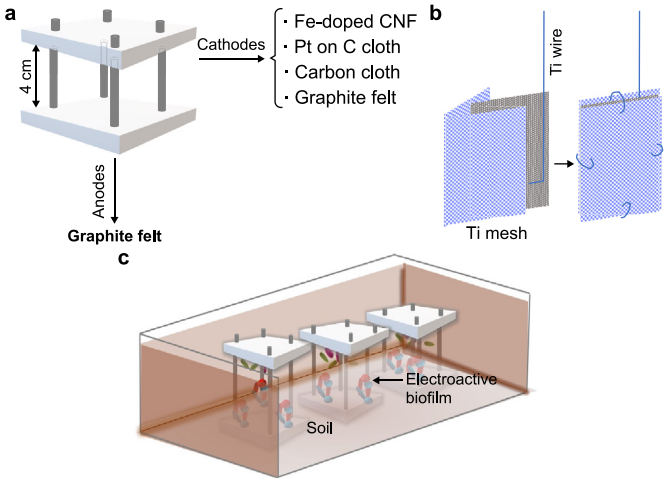

Fig. 1. a, Design and electrode materials of the four SMFCs tested in this study. **b**, Cathode assembly. **c**, Experimental set-up.

2.5. Microbial community analysis

Microbial community analysis of the anodic and cathodic biofilms was performed on one of the three replicates for each of the four types of SMFCs tested, with the exception of SMFC-GF cathodes, for which two of the three replicates were analysed. With this purpose, the SMFCs were disassembled after 56 days of the experiment, and the electrodes were cut into 2 × 2 cm pieces. Soil samples collected in close vicinity to the cathode were also analysed. The electrode and soil samples were kept in 2 mL LifeGuard soil preservation solution (Maryland, USA) at −20 °C until DNA extraction. The latter was carried out by using DNeasy PowerSoil Pro Kit (Qiagen). Paired-end amplicon sequencing of the V3–V4 regions (primers 341F and 806R) of the 16S rRNA gene was carried out by Novogene (Cambridge, UK) using the Illumina NovaSeq 6000 platform. The data was processed, and Amplicon Sequence Variants (ASV) were generated using the dada2 pipeline [50]. Downstream analysis was carried out by using R packages phyloseq and vegan [51,52].

2.6. Morphological and elemental (EDS) analysis

Electrode samples before and after operation were characterised by Scanning Electron Microscopy (SEM, Hitachi SU3900) under an acceleration voltage of 7 kV. Energy-dispersive X-ray spectroscopy (EDS) was performed for CNF–Fe electrodes before and after the operation using the same instrument at an accelerating voltage of 10 kV. To fix the biofilm, the electrode samples were immersed in 2.5% glutaraldehyde and 0.1 M phosphate buffer solution for 30 min each and then dehydrated with increasing ethanol concentration from 30% to 100% for 15 min each [53]. The samples were then dried overnight in a vacuum and sputter coated using a turbomolecular pumped coater (Quorum Q150T Plus) with a 2-mm gold layer before the microscope analysis.

3. Results and discussion

3.1. Electrochemical results

The output voltage generated over time by the four types of SMFCs was compared. Fig. 2a shows the output voltage generated by the SMFCs. The biofilm enrichment and voltage stabilization time may greatly vary in microbial fuel cells, depending on the experimental conditions and design, and it can extend up to several weeks [54]. Incorporating a corrosion-resistive current collector, such as Ti mesh, with carbon electrodes is a promising strategy to improve electrode conductivity [55]. In our work, the use of Ti mesh improved the overall performance without directly contributing to the current generation, as demonstrated by a control study in which the cathode consisted of Ti mesh only (Fig. S4). As shown, the use of carbon cloth as the cathode led to the poorest performance; the output voltage generated by SMFC-CC reached a steady state voltage of 0.086 ± 0.03 V, reached after 10 days of operation. The performances of SMFC-CNFFe and SMFC-PtC were very similar, with steady output voltages of 0.241 ± 0.038 and 0.244 ± 0.033 V, respectively, which remained stable over approximately 40 days,

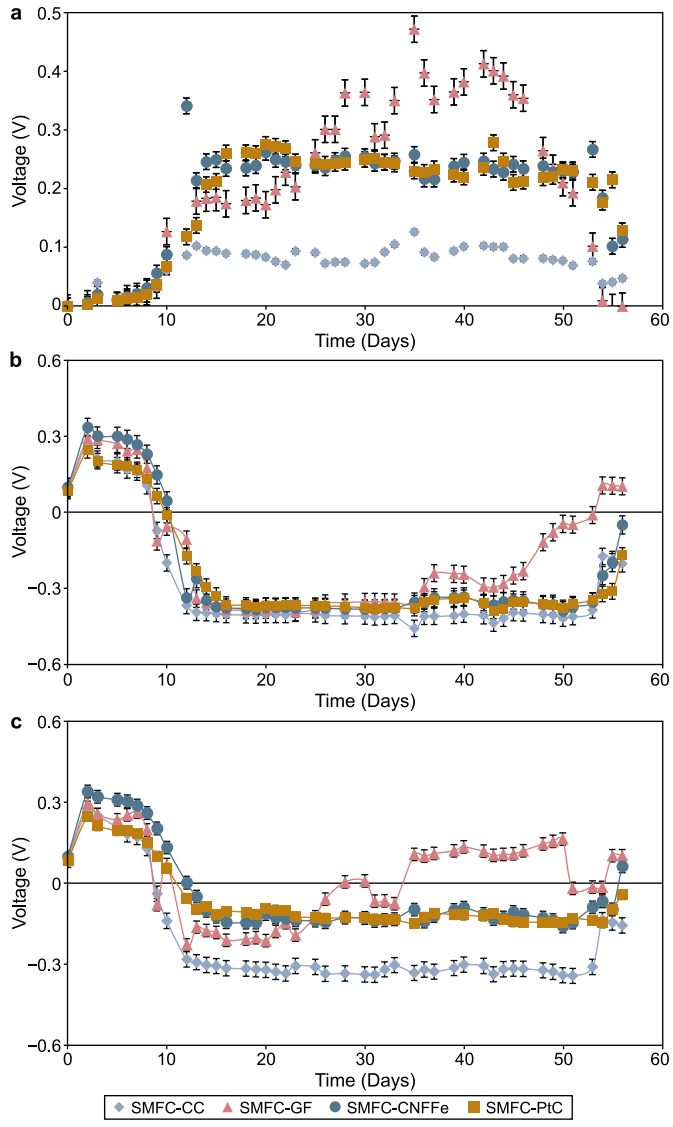

Fig. 2. SMFC performance. **a**, Output voltage generated by the four SMFCs. **b**, Anode potential over time. **c**, Cathode potential over time. Data represent the average of three replicates, and error bars represent the standard error of the mean.

suggesting a consistent electrocatalytic activity. A different trend in the evolution of the output voltage over time was observed in SMFC-GF. In this case, the output voltage initially stabilised at 0.25 ± 0.08 V; however, a second exponential increase in voltage was observed, reaching a second steady value of 0.36 ± 0.06 V after about 25 days of operation. This trend has usually been observed by us with graphite felt cathodes, and an in-depth investigation on the related causes has been discussed in Ref. [56]. Despite the higher output voltage obtained, the performance of SMFC-GF was not stable, and large fluctuations were observed, especially during and after the second exponential increase. As shown in Fig. 2b, the anode performance was not affected by the cathode material, thus confirming that the difference in the overall performance of the several SMFC designs tested largely depended on the cathode, which is consequently the limiting electrode in the system [49]. Fig. 2b shows that after about 10 days of operation, the anode potential vs Ag/AgCl stabilises at −0.365 ± 0.024 V (for SMFC-CNFFe), −0.355 ± 0.043 V (for SMFC-PtC), −0.408 ± 0.014 V (for SMFC-CC), and −0.287 ± 0.11 V (for SMFC-GF). The cathode potentials (Fig. 2c) of CNF−Fe and PtC were similar (−0.121 ± 0.031 and −0.123 ± 0.02 V, respectively), while the cathode potentials for carboncloth was −0.321 ± 0.014 V, suggesting a limited cathodic activity. In the case of SMFC-GF, the average cathode potential reflected the overall fuel cell output voltage trend and, accordingly, is characterised by two stages. A first steady potential value of −0.177 ± 0.045 V was reached after 13 days, remaining stable until day 26. Afterwards, the cathode potential increased to 0.077 ± 0.08 V on day 28. The superior performance of graphite felt as cathode over other materials has been previously demonstrated and attributed to the very high specific surface area of the material that favours biofilm growth [57]. In particular, graphite felt has been shown to facilitate the proliferation of oxygen-reducing microbial communities at the cathode [57]. On the other hand, the graphite-felt cathode led to the most unstable performance of the SMFC, as shown by the large variability in the measurements. Earlier studies with biocathodes also reported a slow increment in the cell voltage and subsequent slow stabilization, attributed to a slow bacterial growth onto the cathode surface [58–60].

For all four types of SMFC, after about 50 days, an increase in both the anode and the cathode potential was observed, which led to a decrease in the output voltage generated. This decline could be attributed to a local decrease in the organic matter available to the biofilm on the electrode surface. This decrease was more pronounced in the SMFC-GF.

The polarization and power curves in tests performed after 27 days of operation (Fig. 3) confirm the superior performance of the SMFC-GF, with a peak power nearly three times higher than the peak power generated by SMFC-PtC and 3.4 times the power generated by SMFC-CNFFe. In particular, SMFC-GF generated a peak power of 0.43 ± 0.009 mW, corresponding to a power density of

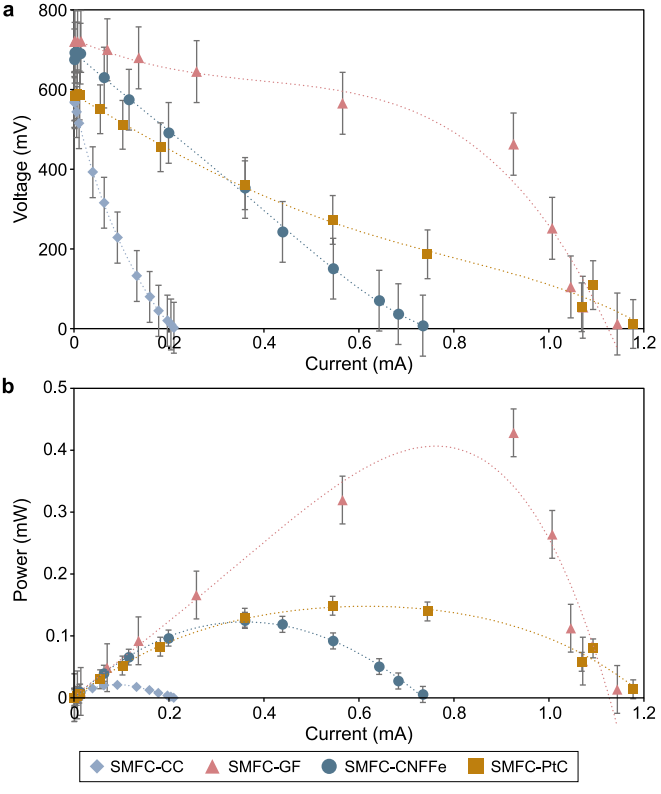

Fig. 3. Polarization tests after 27 days of operation. **a**, Polarization curves; **b**, Power curves. Values are the average of triplicates, and error bars represent the standard error of the mean.

87.3 mW m^{-2} compared to 0.15 ± 0.025 mW (power density 30.4 mW m^{-2}) generated by SMFC-PtC, and 0.127 ± 0.026 mW (power density 25.5 mW m^{-2}) generated by SMFC-CNFFe (Fig. 3b). The lowest power was generated by SMFC-CC (0.021 mW, with a power density 4.285 mW m^{-2}), approximately 95% lower than SMFC-GF, and 86% and 83% lower than the SMFC-PtC and SMFC-CNFFe respectively. The power densities obtained in our study are comparable or, in some cases, higher than those previously reported for SMFCs, which range from 22.9 [40] to 73.5 mW m^{-2} [44]. Our study reports a power density of 87.3 mW m^{-2}, which is, to the best of our knowledge, the highest reported for a single chamber, individual SMFC operated without the addition of any external substrate. The power density value for the CNFFe electrode is 25.5 mW m^{-2}, comparable to values obtained with other catalyst-coated electrodes, including Pt, ranging between 0.85 [42] and 39 mW m^{-2} [46].

To date, no study provides a direct comparison between the use of PtC and CNF–Fe at the cathode of an SMFC. Nevertheless, previous studies confirmed the benefits of using modified CNF at the cathode of microbial fuel cells with surface power densities of up to 60 mW m^{-2} [30] and volumetric power densities of up to 14.4 W m^{-3} [23]. Electrospun N–CNF reported a power density of around 125 mW m^{-2} in a liquid anolyte single-chamber microbial fuel cell [28]. These studies, however, refer to liquid microbial fuel cells (usually operated with synthetic media), with the electrodes physically separated by an ion exchange membrane, which makes a direct comparison impracticable. The much lower electrical conductivity of the soil used in this study (710 μS cm^{-1} compared to 20 mS cm^{-1} for a phosphate buffer-based electrolyte) is a reason for the lower output power generated by SMFC-CNFFe.

The EDS analysis (Fig. S5) suggests that the Fe content of the CNF–Fe cathode did not decrease much with over 50 days of continuous operation: 4.74 wt% initially compared to 3.49 wt% at the end of the experiment. Although the accuracy of this analysis is low, and other components from soil were detected, this result still indicates the long-term stability of the CNF–Fe electrode. Future studies may be directed towards understanding the stability of the electrodes under different operating conditions. SEM images of the four cathodes, before and after the operation, show the presence of a biofilm in each case (Fig. 4). Due to the finer structure of CNF and the large specific surface area of the nanostructure used, greater microbial colonization onto the CNF–Fe electrode surface can be observed.

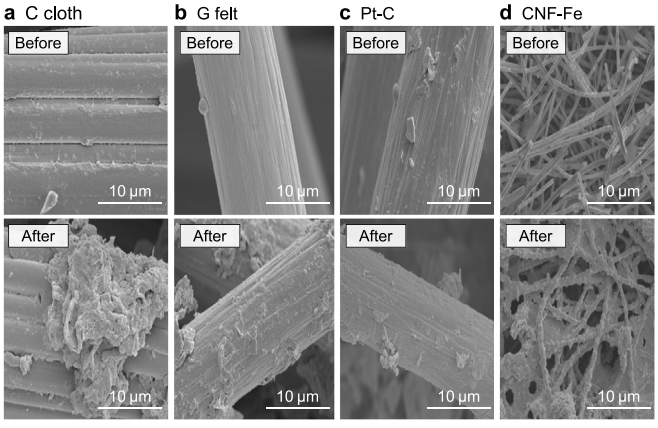

Fig. 4. Morphological analysis by SEM of the electrodes before and at the end of the experiment. The figure shows SEM of cathode electrodes before and after the experiment: **a**, carbon cloth; **b**, graphite felt; **c**, Pt-doped carbon cloth; **d**, CNF–Fe. Acceleration voltage: 7 kV. Magnification: 5000X.

The I–V curve for SMFC-GF indicates a reduced activation loss in the lower current region but an increased concentration loss in the higher current (low resistance) region (Fig. 3a). Aerobic metabolism at the cathode decreases the activation energy at higher resistances by enhancing the final reduction reaction [61]; however, the concentration loss in the lower resistances suggests that the electrons discharged at the anode are not reduced sufficiently fast at the cathode [62]. It has also been previously reported that microbial fuel cells with carbon cloth cathodes suffer from high activation losses and ohmic losses due to poor microbial activity and the absence of catalysts [63]. The polarization curves for CNF–Fe and PtC suggest that there is almost a linear drop in the current, mainly attributed to ohmic losses, which is lower than in the case of non-doped electrodes; however, no major concentration loss can be detected. The ohmic loss can be attributed to the restricted ionic conductivity between anodic and cathodic electrolytes due to the low conductivity of the soil [64]. Although the graphite felt cathode is able to reduce the activation losses due to improved microbial activity and efficient cathode reduction reactions, it suffers from concentration losses that could be alleviated by, for instance, surface functionalization.

EIS tests were performed on the SMFCs at the beginning and the end of their operation by configuring the cathode as the working electrode. As shown in Fig. 5, the ohmic resistance (R_Ω) significantly differs for the four SMFC designs. At the start of the experiment, R_Ω values for all the electrodes (solid symbols in Fig. 5) varied between 295 and 409 Ω, with the lowest value (295 Ω) observed for SMFC-PtC and the highest (409 Ω) value observed for SMFC-CC. Values of different circuit elements are reported in Table 1. Since the SMFCs were operated with the same electrolyte (soil) and moisture content, the observed differences can be attributed primarily to the different electrode materials used for the cathodes. At the end of the experiment, R_Ω values significantly decreased for all the SMFC systems tested (Table 1). This reduction indicates the improved conductivity of the electrodes and soil, likely caused by the formation of an electroactive biofilm on the surface of both the anode and cathode [65]. The equivalent circuit model shows that R2 (R_{ct}),

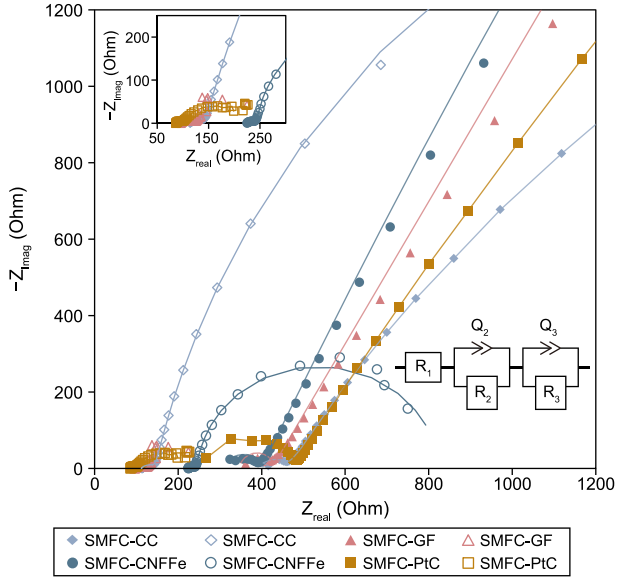

Fig. 5. Nyquist plots of the SMFCs at the start (day 0) and the end (day 54) of the experiment. Solid symbols correspond to data at the start of the experiment, and empty symbols to data at the end of the experiment. Solid lines show the fitting of the equivalent circuit model (ECM) to the data. The inset figure shows an expanded graph for the high-frequency region of day 0.

Table 1
Values of different circuit elements after fitting the ECM to the Nyquist plots.

Cathode material	R1 (Ω)		R2 (Ω)		R3 (Ω)	
	Day 0	Day 54	Day 0	Day 54	Day 0	Day 54
Carbon cloth	409	111.7	45	33.3	-	-
Graphite felt	347.6	92.16	77	27.7	-	-
CNF–Fe	310.1	223.8	89.5	20.6	-	792
Pt-doped carbon cloth	295.6	87.3	196	14.3	-	198

associated with the diameter of the first semicircle, varied between different electrodes at day 0 and was comparatively higher for the catalyst-coated electrodes. We assume that the initial high charge transfer resistance for PtC in this study may be due to operational fluctuations and poor connectivity. After 56 days of operation, the decrease in charge transfer resistance decreased in the following order: PtC (14.3 Ω) < CNF–Fe (20.6 Ω) < Graphite felt (27.7 Ω) < Carbon cloth (33.3 Ω), suggesting that the catalyst-coated electrodes established better connectivity and exhibited better electrocatalytic activity since the biofilm formation decreases the charge transfer resistance [65–67]. Semicircles in the high-frequency region were followed by near linear segments in the low-frequency region due to diffusion resistance, signifying the diffusion process of oxygen in the electrode-electrolyte interface (R3) [57]. After 56 days of operation, the total impedance decreased for all the electrodes (Fig. 4). Moreover, after this time, the effect of diffusion resistance, which is defined by the linear portion in the low-frequency region [30], was no longer observed for SMFC-CNF-Fe and SMFC-PtC (and reduced for SMFC-GF), and instead, closed depressed semicircles were observed for these SMFCs. This result suggests better oxygen diffusion at the electrode-soil interface. Overall, the observed decrease in the total resistance suggests a better charge transfer efficiency and ORR rates due to the formation of an electroactive biofilm onto the surface of the cathode. The graphite-felt cathode led to the lowest total resistance, in agreement with earlier findings [30].

The cyclic voltammetry studies reveal interesting findings about the electrochemical behaviour of the four cathodes tested (Fig. 6). For all four SMFCs, the redox currents obtained at day 0 are very low (Fig. 6b). SMFC-GF showed a reduction current of -3×10^{-5} A and an oxidation current lower than 1×10^{-5} A, while SMFC-CNFFe was characterised by a reduction current of approximately -6×10^{-5} A and an oxidation current of about 1.3×10^{-5} A. The capacitive behaviour of the carbon cloth electrode is indicative of the lack of redox reactions mediated by microbial species and is in line with previously reported results [68].

CV tests at the end of the experiment (day 54) revealed higher peak current values (Fig. 6a), which increased by a factor of 10^2. This result confirms that the formation of a cathodic biofilm enhanced the charge transfer kinetics. Previous studies also showed improved catalytic current values after the formation of an electroactive biofilm in biocathodes [57]. SMFC-CC showed the poorest performance, with a reduction current of around -1×10^{-3} A and an oxidation current of around 0, followed by SMFC-CNFFe (approximately 1.5×10^{-3} to -3×10^{-3} A). On the other hand, SMFC-PtC and SMFC-GF showed the best performance, with an observed oxidation current between 2×10^{-3} and 4×10^{-3} A and a reduction current between -7×10^{-3} and 8×10^{-3} A. These results suggest that, similarly to PtC, the electroactive cathodic biofilm that develops onto the graphite felt plays an important role in ORR reactions and electron transfer processes. Moreover, for the graphite felt electrodes, a pair of quasi-reversible redox peaks at around +0.41 and −0.1 V were observed, suggesting a redox reaction on the electrode. The higher surface area of graphite felt

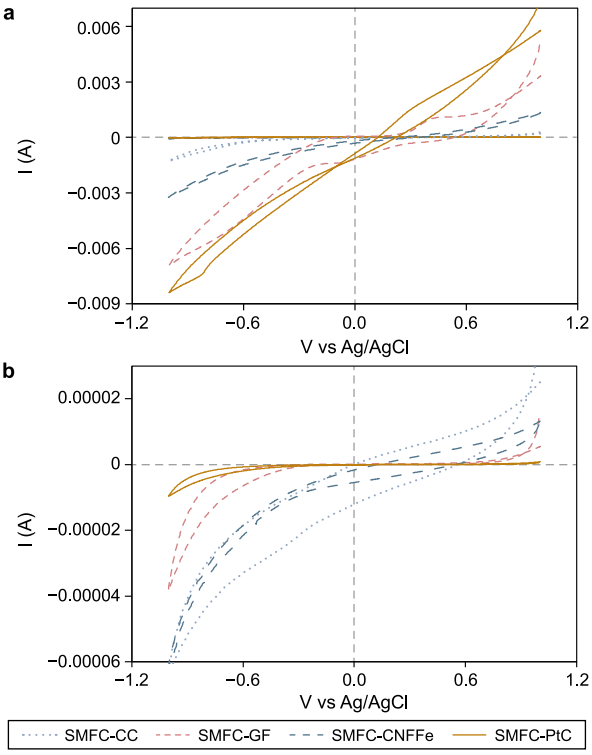

Fig. 6. Cyclic voltammograms of the four cathodes. **a**, Comparing results at the start (day 0) and the end (day 54) of the experiment; **b**, Zoom in on day 0.

enables a better biofilm attachment, resulting in higher ORR activity. The appearance of a pair of distinct redox peaks at around +0.2 and −0.1 V, with CV tests carried out in both air and nitrogen-saturated catholyte in microbial fuel cells with a graphite felt cathode, have been previously associated with the presence of a cathodic biofilm [57].

3.2. Taxonomic analysis of microbial communities

The cathode material may affect the composition of the microbial biofilms colonizing the surface of both the anode and cathode. To evaluate this effect, taxonomic analysis was performed by amplicon sequencing of the 16S rRNA genes of the bacteria in the different communities. Samples were taken from the cathode and anode of each type of SMFC and the soil in the vicinity of the cathode. Since SMFC-GF outperformed the SMFCs with other cathode materials, a duplicate SMFC-GF cathode was also sequenced to evaluate this observation. Analysis of the amplicon data revealed the microbial taxa present at each sampling location (Fig. 7). For each SMFC type tested in the anodic biofilm, the ASVs with the highest relative abundance were members of the family Geobacteraceae (range 5.7–36.2%), followed by the genera *Pseudomonas* (6.2–26.1%), *Geobacter* (5.8–11.0%), and *Bacteroides* (2.1–23.8%); the family Xanthobacteraceae (5.5–8.8%); the genera *Udaeobacter* (3.1–5.8%) and *Faecalibacterium* (0.0–9.8%); *WCHB1-31* from the phylum Bacteriodota (1.6–5.5%), and *Citrifermentans* (1.5–4.8%); and an unidentified Gammaproteobacteria (1.6–4.0%).

The cathode biofilms were dominated by the ASV identified as the unknown Gammaproteobacterium also observed on the anodes (10.9–21.6%), followed by members of the genus *Methylobacterium/Methylorubrum* (1.5–16.9%); the family Xanthobacteraceae (5.2–11.5%); the genera *Hydrogenophaga* (2.8–11.2%), *Methyloversatilis* (2.1–12.0%), *Hyphomicrobium* (1.9–11.7%), *Bacteroides*

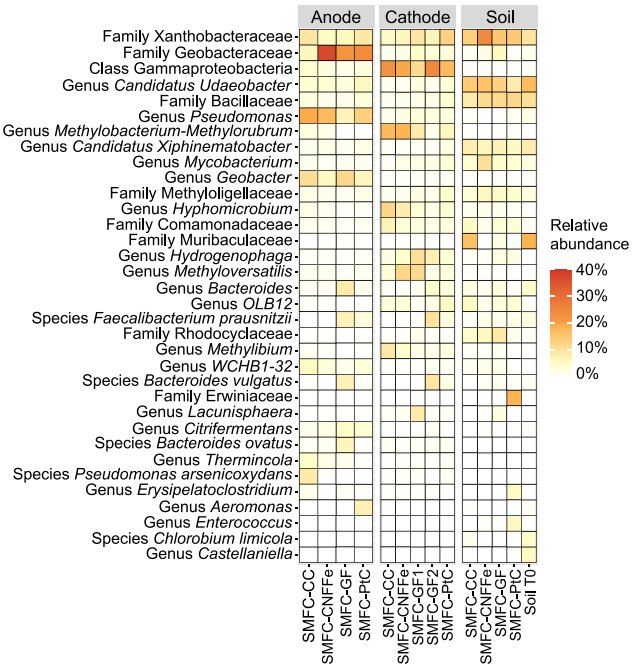

Fig. 7. Heatmap showing the relative abundances of amplicon sequence variants (ASV) detected in each sample, grouped by sample type (anodes, cathodes, and soils in the vicinity of the cathode). Soil T0 refers to the soil used for inoculation of the SMFCs. ASVs with relative abundance >2% present in at least one sample are shown at the lowest taxonomic rank assigned for each ASV.

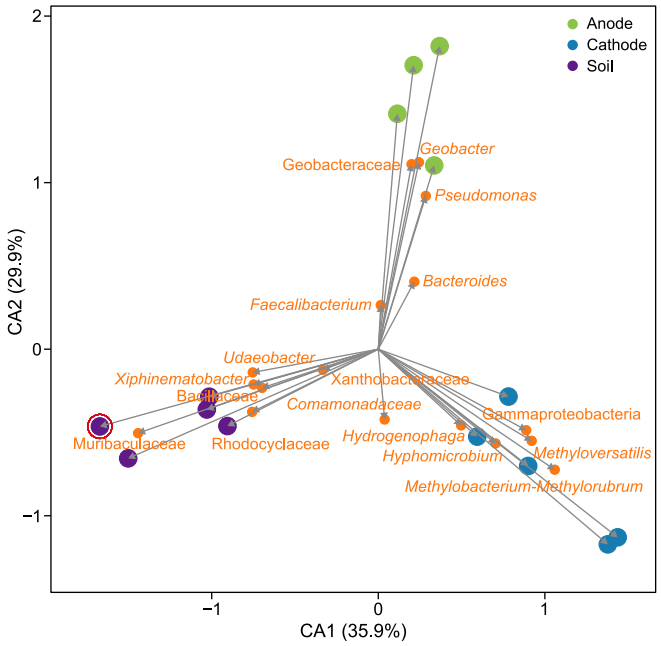

Fig. 8. Canonical Correspondence Analysis (CCA) plot showing the association of taxa with anode, cathode, and soil samples. The red circle indicates time "0" (initial) soil sample.

(0.9–14.7%), *Nitrospira* (1.9–8.2%), and *Methylibium* (1.6–8.9%); the family Comamonadaceae (1.9–6.7%); the genera *Pseudomonas* (2.4–4.1%), *Faecalibacterium* (0.1–10.8%), and *OLB12* from the family Microscillaceae (1.2–3.2%), the families Geobacteraceae (1.7–4.6%) and Methyloligellaceae (1.4–4.0%), and the genera *Mycobacterium* (1.1–3.9%) and *Lacunisphaera* (0.4–8.1%).

The most prevalent taxa in the soil used for inoculation of the SMFCs included the family Muribaculaceae (16.9%), the genera *Udaeobacter* (15.8%), *Bacteroides* (10.8%), the families Bacillaceae (9.7%) and Xanthobacteraceae (8.8%), the genera *Candidatus Xiphinematobacter* (7.5%), *Castellaniella* (6.4%), and *Chlorobium* (4.7%). Interestingly, after the experiment, the soil near each cathode showed a similar microbial composition to the soil at day 0. The most abundant ASVs in the soil near the cathodes included the families Xanthobacteraceae (13.0–23.4%) and Bacillaceae (8.1–11.5%), the genera *Candidatus Udaeobacter* (8.0–15.4%), *Candidatus Xiphinematobacter* (5.4–7.6%), and *Mycobacterium* (4.5–10.8%); the families Rhodocyclaceae (1.7–8.4%), Methyloligellecaea (3.8–5.9%), Muribaculaceae (0.0–15.7%), and Erwiniaceae (0.0–17.8%), and the genera *Bacteroides* (2.8–6.2%).

Canonical Correspondence Analysis (CCA) was carried out to determine which taxa clustered with anodes, cathodes, and soil samples (Fig. 8). The microbial composition of the samples was found to be unique for each sampling location, suggesting selective enrichment on the anodes and cathodes throughout the experiment. The family Geobacteraceae and the genera *Geobacter* and *Pseudomonas* highly correlated with anodes. Both *Geobacter* and *Pseudomonas* are well-known electroactive species; *Geobacter sulfurreducens* is a model organism for direct electron transfer from cell to anode [69], while *Pseudomonas* spp. are known to produce redox compounds that may mediate the transfer of electrons to the anode by other members of the community [70,71]. In addition to *Geobacter* and *Pseudomonas,* a lower enrichment of *Citrifermentans* was also observed across the anode samples. This genus belongs to the family of Geobacteraceae and has been suggested to partake in exoelectrogenic processes [6,72]. Other electroactive taxa were found to be associated with the anodes; however, their presence was not ubiquitous to all SMFCs. These include *Aeromonas* in the case of SMFC-PtC and *Faecalibacterium* in the case of SMFC-GF and SMFC-PtC. Both genera have shown to be electroactive [73,74]. In addition, the genus *Bacteroides* was also found to be enriched in the anodic biofilm of SMFC-GF. *Bacteroides* have been previously detected in anodic biofilms, suggesting they may exhibit an electrochemical function [75,76].

While the relative abundances of species were consistent across the anodic biofilms, the several cathodes presented a different community profile with more variation, possibly as a result of the difference in the cathode material (Fig. 7). On the other hand, the soil near the cathode was associated with a unique set of taxa, which clustered with the initial soil used for inoculum, and not with the cathode electrodes (Fig. 8), suggesting that cathodic enrichment was limited to the electrode's surface.

To determine the effect of cathode material on microbial composition, CCA was carried out for the cathode samples only (Fig. 9). Taxa found enriched on the cathodic biofilms included facultative denitrifiers, electroactive species, as well as hydrogen-producing and hydrogenotrophic bacteria.

The facultative denitrifiers *Methylobacterium/Methylorubrum*, *Hyphomicrobium, Methyloversatilis*, *Hydrogenophaga*, and Comamonadaceae are able to reduce both nitrate and oxygen as the final electron acceptor, and all have been previously detected in cathodic biofilms in liquid microbial fuel cells [77–85]. Electroactive species were also detected on the cathodes, such as *Faecalibacterium* and *Geobacter*, albeit to a lesser extent than on the anodes.

Several hydrogenotrophic taxa were observed on the cathodes, capable of using H_2 as an energy source. However, their abundance varied depending on the cathode material. *Methylobacterium* was associated with CNF–Fe and CC cathodes, *Hydrogenophaga* with GF cathodes, and *Methyloversatilis* with both CNF–Fe and GF cathodes. *Hydrogenophaga* harbour membrane-bound hydrogenases capable

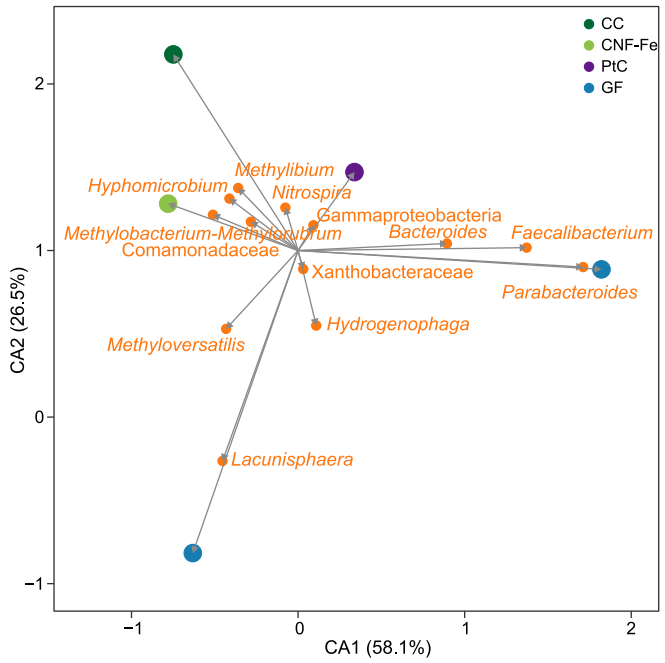

Fig. 9. Canonical Correspondence Analysis (CCA) plot showing the association of taxa with different types of cathode materials used. CC: Carbon cloth; CNF–Fe: Carbon nanofibre doped with iron; PtC: Carbon cloth doped with platinum; GF: Graphite felt (two replicates: GF1 and GF2).

of catalysing both H_2 evolution and oxidation [86], while *Methylobacterium* was reported to produce formate from CO_2, utilizing electrons from a cathode [87]. Similarly, the presence of *Methyloversatilis* was reported to positively correlate with the availability of H_2 [88], as well as with microbial corrosion of carbon steel [89], suggesting that this genus is also able to utilise H_2 to generate reducing power.

Considering the taxonomic composition of the cathodes, we hypothesise that H_2 evolution and oxidation are important mechanisms of electron transfer from cathodes to the biofilm via membrane-bound uptake hydrogenases. It has also been suggested, in the case of liquid-microbial fuel cells, that extracellular hydrogenases and formate dehydrogenases are involved in electron transfer via rapid metabolite cycling [90]. Thus, cathodic environments would favour the enrichment of taxa harbouring such enzymes. The presence of hydrogenotrophs in the cathode biofilms may be associated with improved cathodic activity and overall SMFC performance since the rate of H_2 consumption at the cathode may determine the rate of H_2 evolution from the cathode [91].

The only taxon strongly associated with both replicates of the best-performing GF cathodes was the genus *Hydrogenophaga*. The greater redox activity observed in the case of SMFC-GF (Fig. 5) may indicate an improved capacity of the bacterial communities to accept electrons directly from the cathode to catalyze the oxygen reduction reaction [92], which could be attributed to the greater enrichment of *Hydrogenophaga* on these cathodes [93].

Other taxa were found enriched on either but not both SMFC-GF replicates, including *Lacunisphaera* (SMFC-GF1) and *Faecalibacterium*, *Bacteroides*, and *Parabacteroides* (SMFC-GF2). Of these genera, *Bacteroides* have been reported to produce hydrogen [94,95], whereas the ability to reduce nitrate was reported for both *Lacunisphaera* and *Bacteroides* [96,97]. Since the redox potential of the NO_3^-/NO_2^- couple is +421 mV, likely, the peaks at 419 ± 20 mV observed for SMFC-GF in the CV tests (shown in Fig. 5) are due to the microbial reduction of nitrate to nitrite under aerobic conditions [98]. This result suggests that the enrichment of denitrifiers in the SMFC-GF cathode biofilms, specifically *Hydrogenophaga*, *Lacunisphaera*, and *Bacteroides*, may have facilitated nitrate reduction reaction.

Despite the variability of taxa across different cathodes, an unidentified Gammaproteobacterium was the most prevalent ASV in all cathodic samples. Although the presence of this ASV was low in the inoculum (0.4%), it was enriched not only in the cathodic biofilms of all SMFCs (10.9–21.6%), but also in the anodic biofilms, albeit to a lesser extent (1.6–4.0%). The nucleotide sequence of this ASV was searched against the NCBI database using the BLAST tool, which returned a hit with 100% homology: the sequence of this uncultured bacterium was previously detected in paddy soil microbial fuel cells [99]. In addition, unclassified Gammaproteobacteria were previously reported to dominate biofilms of high-performing oxygen-reducing cathodes [85]. Due to its ubiquity in electrode biofilms in this experiment, it can be hypothesised that this uncultured Gammaproteobacterium is involved in electrochemical processes, particularly in the cathodic biofilm.

4. Conclusions

Understanding the influence of electrode material on the microbial communities involved in the electrogenic processes (and consequently, on the electrochemical performance) is essential to accelerate the translation of SMFCs into practical implementations. This study provides for the first time an in-depth investigation on the effect of different cathode materials on SMFC performance, combining electrochemical analyses with advanced microbial profiling. The use of an innovative CNF–Fe cathode led to an electrochemical performance similar to Pt-doped carbon cloth, thus providing an excellent low-cost alternative. Nonetheless, graphite felt showed better performance than all the other electrodes tested. Not only it exhibited higher voltages, catalytic activity, and lower resistance values, but it also favoured the enrichment of *Hydrogenophaga,* which potentially led to the improvement of cathodic activity by increasing electron uptake via H_2 evolution and/or facilitating nitrate reduction. On the other hand, graphite felt showed much lower reproducibility in results and higher mass transport losses, which might be related to the lack of an oxygen reduction reaction catalyst. Microbial taxonomic profiling of the cathode biofilms revealed taxa related to oxygen reduction or involved in utilizing alternative electron acceptors other than oxygen, such as nitrate. An uncultured Gammaproteobacterium was the most prevalent taxon on all cathode biofilms tested, indicating its importance in drawing electrons from the cathode. Overall, the results generated with this study can inspire future research on low-cost and high-performing SMFCs for practical applications in energy harvesting and bioremediation.

CRediT authorship contribution statement

Arpita Nandy: Conceptualization, Data curation, Formal analysis, Investigation, Methodology, Validation, Visualization, Writing - Original Draft, Writing - Review & Editing. **Daniel Farkas:** Data curation, Formal analysis, Investigation, Methodology, Validation, Visualization, Writing - Original Draft, Writing - Review & Editing. **Belén Pepió-Tárrega:** Formal analysis, Investigation, Methodology, Writing - Original Draft. **Sandra Martinez-Crespiera:** Writing - Review & Editing. **Eduard Borràs:** Funding acquisition, Project administration, Supervision, Writing - Review & Editing. **Claudio Avignone-Rossa:** Funding acquisition, Project administration, Supervision, Writing - Review & Editing. **Mirella Di Lorenzo:** Conceptualization, Funding acquisition, Project administration, Supervision, Validation, Visualization, Writing - Review & Editing.

Declaration of competing interest

The authors declare that they have no known competing interests that could have appeared to influence the work reported in this paper.

Acknowledgements

This research was supported by the EU Horizon 2020 project GREENER (Grant Agreement No 826312). The authors wish to thank: Jakub Dziegielowski and Bongkyu Kim, from the University of Bath, for their suggestions and help on assembling and setting-up the SMFCs; Anna Salvian and Simone Krings, from the University of Surrey, for their assistance in DNA extraction.

Appendix A. Supplementary data

Supplementary data to this article can be found online at https://doi.org/10.1016/j.ese.2023.100276.

References

[1] J. Dziegielowski, B. Metcalfe, M. Di Lorenzo, Towards effective energy harvesting from stacks of soil microbial fuel cells, J. Power Sources 515 (2021), 230591.
[2] L.F.W. Roesch, R.R. Fulthorpe, A. Riva, G. Casella, A.K.M. Hadwin, A.D. Kent, et al., Pyrosequencing enumerates and contrasts soil microbial diversity, ISME J. 1 (2007) 283–290.
[3] A. Wolińska, Z. Stępniewska, A. Bielecka, A, et al., Bioelectricity production from soil using microbial fuel cells, Appl. Biochem. Biotechnol. 173 (2014) 2287–2296, 2014.
[4] A. Bot, J. Benites, The Importance of Soil Organic Matter: Key to Drought-Resistant Soil and Sustained Food Production, FAO Soil Bulletin No. 80, Rome, 2005. FAO.
[5] H. Deng, Yi-C Wu, F. Zhang, Z.-C. Huang, Z. Chen, H.-J. Xu, F. Zhao, Factors affecting the performance of single-chamber soil microbial fuel cells for power generation, Pedosphere 24 (3) (2014) 330–338.
[6] R. Li, J. Wang, T. Li, Q. Zhou, Recent Advances in Improving the Remediation Performance of Microbial Electrochemical Systems for Contaminated Soil and Sediments, Crit Rev Environ Sci Technol, 2022.
[7] S.Z. Abbas, M. Rafatullah, Recent advances in soil microbial fuel cells for soil contaminants remediation, Chemosphere 272 (2021), 129691.
[8] M. Tucci, C.C. Viggi, A.E. Núñez, A. Schievano, K. Rabaey, F. Aulenta, Empowering electroactive microorganisms for soil remediation: challenges in the bioelectrochemical removal of petroleum hydrocarbons, Chem. Eng. J. 419 (2021), 130008.
[9] J. Dziegielowski, B. Metcalfe, P. Villegas-Guzman, C.A. Martínez-Huitle, A. Gorayeb, J. Wenk, M. Di Lorenzo, Development of a functional stack of soil microbial fuel cells to power a water treatment reactor: from the lab to field trials in North East Brazil, Appl. Energy 278 (2020), 115680.
[10] B. Min, B.E. Logan, Continuous electricity generation from domestic wastewater and organic substrates in a flat plate microbial fuel cell, Environ. Sci. Technol. 38 (2004) 5809.
[11] F. Papiya, A. Nandy, S. Mondal, P.P. Kundu, Co/Al2O3-rGO nanocomposite as cathode electrocatalyst for superior oxygen reduction in microbial fuel cell applications: the effect of nanocomposite composition, Electrochim. Acta 254 (2017) 1–13.
[12] B.E. Logan, Scaling up microbial fuel cells and other bioelectrochemical systems, Appl. Microbiol. Biotechnol. 85 (2010) 1665–1671.
[13] L. Li, M. Wang, N. Cui, Y. Ding, Q. Feng, W. Zhang, X. Li, CeO2 doped Pt/C as an efficient cathode catalyst for an air-cathode single-chamber microbial fuel cell, RSC Adv. 6 (2016), 25877.
[14] L. Deng, M. Zhou, C. Liu, L. Liu, C. Liu, S. Dong, Development of high performance of Co/Fe/N/CNT nanocatalyst for oxygen reduction in microbial fuel cells, Talanta 81 (2010) 444–448.
[15] G.A. Kovalenko, L.G. Tomashevskaya, T.V. Chuenko, N.A. Rudina, L.V. Perminova, A.N. Reshetilov, Synthesis of catalytic filamentous carbon on a nickel/graphite catalyst and a study of the resulting carbon–carbon composite materials in microbial fuel cells, Kinet. Catal. 52 (2011) 564.
[16] M. Ghasemi, W.R.W. Daud, M. Rahimnejad, M. Rezayi, A. Fatemi, Y. Jafari, M.R. Somalu, A. Manzour, Copper-phthalocyanine and nickel nanoparticles as novel cathode catalysts in microbial fuel cells, Int. J. Hydrogen Energy 38 (2013) 9533–9540.
[17] P. Pattanayak, F. Papiya, V. Kumar, A. Singh, P.P. Kundu, Performance evaluation of poly(aniline-co-pyrrole) wrapped titanium dioxide nanocomposite as an air-cathode catalyst material for microbial fuel cell, Mater. Sci. Eng. C 118 (2021), 111492.
[18] B. Koo, S.P. Jung, Improvement of air cathode performance in microbial fuel cells by using catalysts made by binding metal-organic framework and activated carbon through ultrasonication and solution precipitation, Chem. Eng. J. 424 (2021), 130388.
[19] B. Koo, S. Lee, S. Oh, E.J. Kim, Y. Hwang, D. Seo, J.Y. Kim, Y.H. Kahng, Y.W. Lee, S. Chung, S. Kim, J.H. Par, S.P. Jung, Addition of reduced graphene oxide to an activated-carbon cathode increases electrical power generation of a microbial fuel cell by enhancing cathodic performance, Electrochim. Acta 297 (2019) 613–622.
[20] D.H. Reneker, I. Chun, Nanometre diameter fibers of polymer, produced by electrospinning, Nanotechnology 7 (1996) 216–223.
[21] X. Lu, W. Zhang, C. Wang, T.C. Wen, Y. Wei, One-dimensional conducting polymer nanocomposites: synthesis, properties and applications, Prog. Polym. Sci. 36 (2011) 671–712.
[22] H. Eom, H.J. Joo, S.C. Kim, S.S. Kim, Properties of carbon-based nanofiber with Pd and itsapplication to microbial fuel cells electrode, Environ. Technol. Innov. 19 (2020), 100800.
[23] P. Bosch-Jimenez, S. Martinez-Crespiera, D. Amantia, M.D. Pirriera, I. Forns, R. Shechter, E. Borràs, Non-precious metal doped carbon nanofiber air-cathode for Microbial Fuel Cells application: oxygen reduction reaction characterization and long-term validation, Electrochim. Acta 228 (2017) 380–388.
[24] E. Borràs, M. Aliaguilla, N. Bossa, S. Martinez-Crespiera, L. Huidobro, R. Schweiss, A. Schwenke, P. Bosch-Jimenez, Nanomaterials-based air-cathodes use in microbial desalination cells for drinking water production: synthesis, performance and release assessment, J. Environ. Chem. Eng. 9 (2021), 105779.
[25] Z. Chen, D. Higgins, Z. Chen, Nitrogen doped carbon nanotubes and their impact on the oxygen reduction reaction in fuel cells, Carbon 48 (2010) 3057–3065.
[26] Y. Yuan, B. Zhao, Y. Jeon, S. Zhong, S. Zhou, S. Kim, Iron phthalocyanine supported on amino-functionalized multi-walled carbon nanotube as an alternative cathodic oxygen catalyst in microbial fuel cells, Bioresour. Technol. 102 (2011) 5849–5854.
[27] M. Ghasemi, M. Ismail, S.K. Kamarudin, K. Saeedfar, W.R.W. Daud, S.H.A. Hassan, L.Y. Heng, J. Alam, S.-E. Oh, Carbon nanotube as an alternative cathode support and catalyst for microbial fuel cells, Appl. Energy 102 (2013) 1050.
[28] G. Massaglia, V. Margaria, A. Sacco, M. Castellino, A. Chiodoni, F.C. Pirri, M. Quaglio, N-doped carbon nanofibers as catalyst layer at cathode in single chamber Microbial Fuel Cells, Int. J. Hydrogen Energy 44 (2019) 4442–4449.
[29] P. Dange, N. Savla, S. Pandit, R. Bobba, S.P. Jung, et al., A comprehensive review on oxygen reduction reaction in microbial fuel cells, J Renew Mater 10 (2022) 665–697.
[30] M. Ghasemi, S. Shahgaldi, M. Ismail, B.H. Kim, Z. Yaakob, &W.R. Wan Daud, Activated carbon nanofibers as an alternative cathode catalyst to platinum in a two-chamber microbial fuel cell, Int. J. Hydrogen Energy 36 (2011) 13746–13752.
[31] N. Jiang, M. Huang, J. Li, J. Song, S. Zheng, Y. Gao, M. Shao, Y. Li, Enhanced bioelectricity output of microbial fuel cells via electrospinning zeolitic imidazolate framework-67/polyacrylonitrile carbon nanofiber cathode, Bioresour. Technol. 337 (2021), 125358.
[32] T. Cai, Y. Huang, M. Huang, Y. Xi, D. Pang, W. Zhang, Enhancing oxygen reduction reaction of supercapacitor microbial fuel cells with electrospun carbon nanofibers composite cathode, Chem. Eng. J. 371 (2019) 544–553.
[33] Y. Liu, J. Wang, Y. Sun, H. Li, Z. Zhai, S. Guo, T. Ren, C. Li, Nitrogen-doped carbon nanofibers anchoring Fe nanoparticles as biocompatible anode for boosting extracellular electron transfer in microbial fuel cells, J. Power Sources 544 (2022), 231890.
[34] J.-L. Sanchez, D. Pinto, C. Laberty-Robert, Electrospun carbon fibers for microbial fuel cells: a novel bioanode design applied to wastewater treatment, Electrochim. Acta 373 (2021), 137864.
[35] X. Yu, T. Guo, X. Liu, B. Zhou, X. Zhai, J. Yang, X. Wang, Y. Hou, Q. Yang, Improving surface properties of cathode and increasing abundance of autotrophic bacteria for chromium reduction with amino functionalized carbon nanotubes, J. Environ. Chem. Eng. 10 (2022), 108005.
[36] X. Cao, H.-L. Song, C.-Y. Yu, X.-N. Li, Simultaneous degradation of toxic refractory organic pesticide and bioelectricity generation using a soil microbial fuel cell, Bioresour. Technol. 189 (2015) 87–93.
[37] H. Wang, H. Song, R. Yu, X. Cao, Z. Fang, X. Li, New process for copper migration by bioelectricity generation in soil microbial fuel cells, Environ. Sci. Pollut. Res. 23 (2016) 13147–13154.
[38] N. Habibul, Hu Yi, G.-P. Sheng, Microbial fuel cell driving electrokinetic remediation of toxic metal contaminated soils, J. Hazard Mater. 318 (2016) 9–14.
[39] T.-S. Song, J. Zhang, S. Hou, H. Wang, D. Zhang, S. Li, J. Xie, Electrokinetic remediation of toxic metal-contaminated soil driven by solid phase microbial fuel cells with a wheat straw addition, J. Chem. Technol. Biotechnol. 318 (2018) 9–14.
[40] G. Huang, Y. Zhang, J. Tang, Y. Du, Remediation of Cd contaminated soil in microbial fuel cells: effects of Cd concentration and electrode spacing, J. Environ. Eng. 146 (2020), 04020050.
[41] L. Lu, H. Yazdi, S. Jin, Y. Zuo, P.H. Fallgren, Z.J. Ren, Enhanced bioremediation of hydrocarbon-contaminated soil using pilot-scale bioelectrochemical systems, J. Hazard Mater. 274 (2014b) 8–15.
[42] X. Wang, Z. Cai, Q. Zhou, Z. Zhang, C. Chen, Bioelectrochemical stimulation of

petroleum hydrocarbon degradation in saline soil using U-tube microbial fuel cells, Biotechnol. Bioeng. 109 (2012) 426–433.
[43] D.-Y. Huang, S.-G. Zhou, Q. Chen, B. Zhao, Y. Yuan, L. Zhuang, Enhanced anaerobic degradation of organic pollutants in a soil microbial fuel cell, Chem. Eng. J. 172 (3) (2011) 647–653.
[44] M.I. Simeon, A. Weig, R. Freitag, Optimization of soil microbial fuel cell for sustainable bio-electricity production: combined effects of electrode material, electrode spacing, and substrate feeding frequency on power generation and microbial community diversity, Biotechnol. Biofuels 15 (124) (2022a).
[45] M.I. Simeon, R. Freitag, Influence of electrode spacing and fed-batch operation on the maximum performance trend of a soil microbial fuel cell, Int. J. Hydrogen Energy 47 (2022b) 12304–12316.
[46] L. Lu, T. Huggins, S. Jin, Yi Zuo, Z.J. Ren, Microbial metabolism and community structure in response to bioelectrochemically enhanced remediation of petroleum hydrocarbon-contaminated soil, Environ. Sci. Technol. 48 (7) (2014a) 4021–4029.
[47] S. Monasterio, M. Di Lorenzo, Electricity generation from untreated fresh digestate with a cost-effective array of floating microbial fuel cells, Chem. Eng. Sci. 198 (2019) 108–116.
[48] T. Nam, S. Son, E. Kim, H.V.H. Tran, B. Koo, H. Chai, J. Kim, S. Pandit, A. Gurung, S.-E. Oh, E.J. Kim, Y. Choi, S.P. Jung, Improved structures of stainless steel current collector increase power generation of microbial fuel cells by decreasing cathodic charge transfer impedance, Environ Eng Res 23 (2018) 383–389.
[49] E. Casula, B. Kim, H. Chesson, M. Di Lorenzo, M. Mascia, Modelling the influence of soil properties on performance and bioremediation ability of a pile of soil microbial fuel cells, Electrochim. Acta 368 (2021), 137568.
[50] B.J. Callahan, P.J. McMurdie, M.J. Rosen, A.W. Han, A.J. Johnson, S.P. Holmes, DADA2: high-resolution sample inference from Illumina amplicon data, Nat. Methods 13 (2016) 581–583.
[51] P.J. McMurdie, S. Holmes, phyloseq: an R package for reproducible interactive analysis and graphics of microbiome census data, PLoS One 8 (2013), e61217.
[52] P. Dixon, VEGAN, a package of R functions for community ecology, J. Veg. Sci. 14 (2003) 927–930.
[53] A. Nandy, V. Kumar, S. Mondal, K. Dutta, M. Salah, P.P. Kundu, Performance evaluation of microbial fuel cells: effect of varying electrode configuration and presence of a membrane electrode assembly, N. Biotech. 32 (2015) 272–281.
[54] H.V.H. Tran, E. Kim, S.P. Jung, Anode biofilm maturation time, stable cell performance time, and time-course electrochemistry in a single-chamber microbial fuel cell with a brush-anode, J. Ind. Eng. Chem. 106 (2022) 269–278.
[55] S.P. Jung, E. Kim, B. Koo, B, Effects of wire-type and mesh-type anode current collectors on performance and electrochemistry of microbial fuel cells, Chemosphere 209 (2018) 542–550.
[56] J. Dziegielowski, M. Mascia, B. Metcalfe, M. Di Lorenzo, Voltage evolution and electrochemical behaviour of Soil microbial fuel cells operated in different quality soils, Sustain. Energy Technol. Assessments 56 (2023), 103071.
[57] Y. Zhang, J. Sun, Y. Hu, S. Li, Q. Xu, Bio-cathode materials evaluation in microbial fuel cells: a comparison of graphite felt, carbon paper and stainless steel mesh materials, Int. J. Hydrogen Energy 37 (2012) 16935–16942.
[58] Z. He, L.T. Angenent, Application of bacterial biocathodes in microbial fuel cells, Electroanalysis 18 (2006) 2009–2015.
[59] X. Xia, Y. Sun, P. Liang, X. Huang, Long-term effect of set potential on biocathodes in microbial fuel cells: electrochemical and phylogenetic characterization, Bioresour. Technol. 120 (2012) 26–33.
[60] S.V. Ramanaiah, C.M. Cordas, S.C. Matias, M.V. Reddy, J.H. Leitão, L.P. Fonseca, Bioelectricity generation using long-term operated biocathode: RFLP based microbial diversity analysis, Biotechnol. Rep 32 (2021), e00693.
[61] Y. Li, J. Liu, X. Chen, J. Wu, N. Li, W.Y. Feng, Tailoring surface properties of electrodes for synchronous enhanced extracellular electron transfer and enriched exoelectrogens in microbial fuel cells, ACS Appl. Mater. Interfaces 13 (2021) 58508–58521.
[62] G. Velvizhi, S. Venkata Mohan, Electrogenic activity and electron losses under increasing organic load of recalcitrant pharmaceutical wastewater, Int. J. Hydrogen Energy 37 (2012) 5969–5978.
[63] B.E. Logan, B. Hamelers, R. Rozendal, U. Schröder, J. Keller, S. Freguia, P. Aelterman, W. Verstraete, K. Rabaey, Microbial fuel cells: methodology and technology, Environ. Sci. Technol. 40 (2006) 5181–5192.
[64] M.I. Simeon, F.U. Asoiro, M. Aliyu, O.A. Raji, R. Freitag, Polarization and power density trends of a soil-based microbial fuel cell treated with human urine, Int. J. Energy Res. 44 (2020) 5968–5976.
[65] Z. He, F. Mansfeld, Exploring the use of electrochemical impedance spectroscopy (EIS) in microbial fuel cell studies, Energy Environ. Sci. 2 (2009) 215–219.
[66] A. Nandy, M. Sharma, S.V. Venkatesan, N. Taylor, L. Gieg, V. Thangadurai, Comparative evaluation of coated and non-coated carbon electrodes in a microbial fuel cell for treatment of municipal sludge, Energies 12 (2019) 1034.
[67] S. Jung, Y.-H. Ahn, S.-E. Oh, J. Lee, K.T. Cho, Y. Kim, M.W. Kim, J. Shim, M. Kang, Impedance and thermodynamic analysis of bioanode, abiotic anode, and riboflavin-amended anode in microbial fuel cells, Bull. Kor. Chem. Soc. 33 (10) (2012) 3349.
[68] M.I. Alvarado Avila, E. Toledo-Carrillo, J. Dutta, Improved chlorate production with platinum nanoparticles deposited on fluorinated activated carbon cloth electrodes, Clean. Eng. Tech. 1 (2020), 100016.
[69] G. Reguera, K.D. McCarthy, T. Mehta, J.S. Nicoll, M.T. Tuominen, D.R. Lovley, Extracellular electron transfer via microbial nanowires, Nature 435 (2005) 1098–1101.
[70] K. Rabaey, N. Boon, M. Höfte, M.W. Verstraete, Microbial phenazine production enhances electron transfer in biofuel cells, Environ. Sci. Technol. 39 (2005) 3401–3408.
[71] T.H. Pham, N. Boon, P. Aelterman, P. Clauwaert, L. De Schamphelaire, L. Vanhaecke, K. De Maeyer, M. Höfte, W. Verstraete, K. Rabaey, Metabolites produced by Pseudomonas sp. enable a Gram-positive bacterium to achieve extracellular electron transfer, Appl. Microbiol. Biotechnol. 77 (2008) 1119–1129.
[72] X. Luo, L. Huang, X. Cai, L. Zhou, S. Zhou, Y. Yuan, Structure and Core Taxa of Bacterial Communities Involved in Extracellular Electron Transfer in Paddy Soils across China, Science of The Total Environment 844 (2022) 157196.
[73] C.A. Pham, S.J. Jung, N.T. Phung, J. Lee, I.S. Chang, B.H. Kim, H. Yi, J. Chun, A novel electrochemically active and Fe(III)-reducing bacterium phylogenetically related to Aeromonas hydrophila, isolated from a microbial fuel cell, FEMS Microbiol. Lett. 223 (2003) 129–134.
[74] M.T. Khan, S.H. Duncan, A.J. Stams, J.M. van Dijl, H.J. Flint, H.J. Harmsen, The gut anaerobe Faecalibacterium prausnitzii uses an extracellular electron shuttle to grow at oxic-anoxic interphases, ISME J. 6 (2012) 1578–1585.
[75] A.M. Lakaniemi, O.H. Tuovinen, J.A. Puhakka, Anaerobic conversion of microalgal biomass to sustainable energy carriers–a review, Bioresour. Technol. 135 (2013) 222–231.
[76] P. Izadi, M.N. Gey, N. Schlüter, U. Schröder, Bidirectional electroactive microbial biofilms and the role of biogenic sulfur in charge storage and release, iScience 24 (2012), 102822.
[77] J. Huang, Z. Wang, C. Zhu, J. Ma, X. Zhang, Z. Wu, Identification of microbial communities in open and closed circuit bioelectrochemical MBRs by high-throughput 454 pyrosequencing, PLoS One 9 (2014), e93842.
[78] Q. Liu, B. Liu, W. Li, X. Zhao, W. Zuo, D. Xing, Impact of ferrous iron on microbial community of the biofilm in microbial fuel cells, Front. Microbiol. 8 (2017) 920.
[79] R. Liu, X. Zheng, M. Li, L. Han, X. Liu, F. Zhang, X. Hou, A three chamber bioelectrochemical system appropriate for in-situ remediation of nitrate-contaminated groundwater and its reaction mechanisms, Water Res. 158 (2019) 401–410.
[80] C. Chang, W. Kao, C. Yu, Assessment of voltage reversal effects in the serially connected biocathode-based microbial fuel cells through treatment performance, electrochemical and microbial community analysis, Chem. Eng. J. 397 (2020), 125368.
[81] O. Obata, M.J. Salar-Garcia, J. Greenman, H. Kurt, K. Chandran, I. Ieropoulos, Development of efficient electroactive biofilm in urine-fed microbial fuel cell cascades for bioelectricity generation, J. Environ. Manag. 258 (2020), 109992.
[82] S.V. Ramanaiah, C.M. Cordas, S.C. Matias, M.V. Reddy, J.H. Leitão, L.P. Fonseca, Bioelectricity generation using long-term operated biocathode: RFLP based microbial diversity analysis, Biotechnol Rep 32 (2021), e00693.
[83] C.C. Chang, S.L. Li, A. Hu, C.P. Yu, Long-term operation of bio-catalyzed cathodes within continuous flow membrane-less microbial fuel cells, Chemosphere 266 (2021), 129059.
[84] G. Pierangeli, R. Ragio, R. Benassi, G. Gregoracci, E. Subtil, Pollutant removal, electricity generation and microbial community in an electrochemical membrane bioreactor during co-treatment of sewage and landfill leachate, J. Environ. Chem. Eng. 9 (2021), 106205.
[85] M. Rothballer, M. Picot, T. Sieper, J.B.A. Arends, M. Schmid, A. Hartmann, N. Boon, C.J.N. Buisman, F. Barrière, D.P. Strik, Monophyletic group of unclassified γ-Proteobacteria dominates in mixed culture biofilm of high-performing oxygen reducing biocathode, Bioelectrochemistry 106 (2015) 167–176.
[86] K.S. Yoon, Y. Sakai, N. Tsukada, K. Fujisawa, H. Nishihara, Purification and biochemical characterization of a membrane-bound [NiFe]-hydrogenase from a hydrogen-oxidizing, lithotrophic bacterium, Hydrogenophaga sp. AH-24, FEMS Microbiol. Lett. 290 (2009) 114–120.
[87] H. Hwang, Y.J. Yeon, S. Lee, H. Choe, M.G. Jang, D.H. Cho, S. Park, Y.H. Kim, Electro-biocatalytic production of formate from carbon dioxide using an oxygen-stable whole cell biocatalyst, Bioresour. Technol. 185 (2015) 35–39.
[88] A. Ontiveros-Valencia, Z.E. Ilhan, D.W. Kang, B. Rittmann, R. Krajmalnik-Brown, Phylogenetic analysis of nitrate- and sulfate-reducing bacteria in a hydrogen-fed biofilm, FEMS Microbiol. Ecol. 85 (2013) 158–167.
[89] R. Shrestha, T. Černoušek, J. Stoulil, H. Kovářová, K. Sihelská, R. Špánek, A. Ševců, J. Steinová, Anaerobic microbial corrosion of carbon steel under conditions relevant for deep geological repository of nuclear waste, Sci. Total Environ. 800 (2021), 149539.
[90] J.S. Deutzmann, M. Sahin, A.M. Spormann, Extracellular enzymes facilitate electron uptake in biocorrosion and bioelectrosynthesis, mBio 6 (2015) e00496-15.
[91] J. Philips, Extracellular electron uptake by acetogenic bacteria: does H_2 consumption favor the H_2 evolution reaction on a cathode or metallic iron? Front. Microbiol. 10 (2020) 2997.
[92] P. Izadi, L. F. L. Fernández Jean-Marie Fontmorin, S. Cheng, I. Head, E.H. Yu, High performing gas diffusion biocathode for microbial fuel cells using acidophilic iron oxidizing bacteria, Front. Energy Res. 7 (2019).
[93] A. Willems, J. Busse, M. Goor, B. Pot, E. Falsen, E. Jantzen, B. Hoste, M. Gillis, K. Kersters, G. Auling, J. De Ley, Hydrogenophaga, a New genus of hydrogen-oxidizing bacteria that includes Hydrogenophaga flava comb. Nov. (Formerly Pseudomonas flava), Hydrogenophaga palleronii (formerly Pseudomonas palleronii), Hydrogenophaga pseudoflava (formerly Pseudomonas

pseudoflava and “Pseudomonas carboxy do flava”, and Hydrogenophaga taeniospiralis (Formerly Pseudomonas taeniospiralis), Int J Syst Evol, Microbiol 39 (1989) 319–333.
[94] G. Harding, V. Sutter, S. Finegold, K. Bricknell, Characterization of bacteroides melaninogenicus, J. Clin. Microbiol. 4 (1976) 354–359.
[95] C. Chassard, E. Delmas, P.A. Lawson, A. Bernalier-Donadille, Bacteroides xylanisolvens sp. nov., a xylan-degrading bacterium isolated from human faeces, Int. J. Syst. Evol. Microbiol. 58 (2008) 1008–1013.
[96] Y. Zhao, C. Bu, H. Yang, Z. Qiao, S. Ding, S.-Q. Ni, Survey of dissimilatory nitrate reduction to ammonium microbial community at national wetland of Shanghai, China, Chemosphere 250 (2020), 126195.
[97] I. Yamamoto, T. Mitsui, M. Ishimoto, Nitrate reduction in bacteroides multiacidus: its effect on glucose metabolism and some properties of the reductase, J. Gen. Appl. Microbiol. 28 (1982) 451–463.
[98] M.G. Liebensteiner, N. Tsesmetzis, A.J.M. Stams, B.P. Lomans, Microbial redox processes in deep subsurface environments and the potential application of (per)chlorate in oil reservoirs, Front. Microbiol. 5 (2014).
[99] W. Gustave, Z.F. Yuan, R. Sekar, Y.X. Ren, J.Y. Liu, J. Zhang, Z. Chen, Soil organic matter amount determines the behavior of iron and arsenic in paddy soil with microbial fuel cells, Chemosphere 237 (2019), 124459.